# Loss of Nuclear and Membrane Estrogen Receptor-α Differentially Impairs Insulin Secretion and Action in Male and Female Mice

Camille Allard,[1] Jamie J. Morford,[1,2,3] Beibei Xu,[1] Benjamin Salwen,[1] Weiwei Xu,[1] Lucie Desmoulins,[4] Andrea Zsombok,[3,4] Jason K. Kim,[5] Ellis R. Levin,[6,7] and Franck Mauvais-Jarvis[1,2,3,8]

*Diabetes 2019;68:490–501 | https://doi.org/10.2337/db18-0293*

**Estrogens favor glucose homeostasis primarily through the estrogen receptor-α (ERα), but the respective importance of nuclear ERα (NOER) and membrane ERα (MOER) pools to glucose homeostasis are unknown. We studied glucose homeostasis, insulin secretion, and insulin sensitivity in male and female mice expressing either the NOER or the MOER. Male and female MOER mice exhibited fasting and fed hyperglycemia and glucose intolerance. Female MOER mice displayed impaired central insulin signaling associated with hyperinsulinemia and insulin resistance due to unrestrained hepatic gluconeogenesis, without alterations in glucose-stimulated insulin secretion (GSIS). In contrast, male MOER mice did not exhibit detectable insulin resistance, but showed impaired GSIS associated with reduced brain glucose sensing. Female NOER mice exhibited milder hepatic insulin resistance and glucose intolerance. In conclusion, nuclear ERα signaling is predominant in maintaining glucose homeostasis in mice of both sexes. Lack of nuclear ERα alters the central control of insulin sensitivity in females and predominantly impairs the central regulation of insulin secretion in males.**

Estrogens favor glucose homeostasis, and estrogen deficiency predisposes males and females to dysglycemia (1,2). In women, early menopause (producing prolonged 17β-estradiol [E2] deficiency) and surgical menopause by oophorectomy (producing rapid and severe E2 deficiency) both increase the risk of type 2 diabetes compared with women with natural menopause (2). In men, total estrogen deficiency induced by inactivating mutations of the CYP19 gene, which codes for aromatase, produces insulin resistance, glucose intolerance, and even type 2 diabetes (1). In both cases, estrogen therapy improves metabolic alterations. The metabolic actions of estrogens are mediated via the estrogen receptor (ER)-α (ERα), ERβ, and the membrane-bound G-protein–coupled ER. ERα is believed to account for most actions of estrogens on glucose homeostasis in vivo. Male and female mice with global knockout of ERα (ERαKO) develop insulin resistance and glucose intolerance (3–6). Experimentally, skeletal muscle pools of ERα are more important for systemic insulin action (4,7). The loss of ERα in pancreatic islets also predisposes male and female mice to pancreatic β-cell dysfunction and failure in conditions of metabolic stress (8–10). ERα is a ligand-activated transcription factor that regulates gene expression by binding estrogen response elements present on the DNA or by indirect binding via tethering to other transcription factors (11). ERα is not only localized to the nuclear compartment but is also present in extranuclear locations at the level of membranes. Membrane targeting of ERα through palmitoylation at cysteine residues (12) represents 5–10% of the total pool depending on the cell type (13). Membrane localization of ERα facilitates

[1]Section of Endocrinology and Metabolism, Department of Medicine, Tulane University Health Sciences Center, New Orleans, LA
[2]Neuroscience Program, Tulane University, New Orleans, LA
[3]Brain Institute, Tulane University, New Orleans, LA
[4]Department of Physiology, Tulane University Health Sciences Center, New Orleans, LA
[5]Division of Endocrinology, Metabolism and Diabetes, Department of Medicine, University of Massachusetts Medical School, Worcester, MA
[6]Department of Medicine and Biochemistry, University of California, Irvine, CA
[7]Long Beach VA Medical Center, Long Beach, CA
[8]Southeast Louisiana Veterans Healthcare Medical Center, New Orleans, LA

Corresponding author: Franck Mauvais-Jarvis, fmauvais@tulane.edu

Received 9 March 2018 and accepted 24 September 2018

This article contains Supplementary Data online at http://diabetes.diabetesjournals.org/lookup/suppl/doi:10.2337/db18-0293/-/DC1.



**See accompanying article, p. 471.**

membrane-initiated rapid signaling events that are important in males and females for reproduction (14,15), neuronal function (16), and vascular health (17). The activation of extranuclear ERα also promotes pancreatic islet survival from apoptotic stresses (18), prevents excess islet lipogenesis (9,19), and stimulates insulin synthesis (20). The importance of extranuclear steroid receptors in metabolic homeostasis is not limited to ERs. The androgen receptor also exhibits extranuclear/membrane location in β-cells with a critical role in insulin secretion in males (21). Therefore, understanding the contributions of extranuclear and nuclear pools of ERα to glucose homeostasis is a necessary step toward the development of sex-based therapies in diabetes.

Here, we studied mice of both sexes expressing either the membrane ERα (MOER) or the nuclear ERα (NOER) pools (14,22) to determine their contribution to glucose homeostasis, insulin action, and insulin secretion.

## RESEARCH DESIGN AND METHODS

### Animals

The generation and genotyping of ERαKO (23), MOER (22) and NOER (14) mice were described previously (Fig. 1*A*). MOER mice genotyping confirmed the absence of the endogenous expression of ERα and the presence of the human E domain of ERα (Supplementary Fig. 1*A* and *B*). Moreover, MOER mice and littermate controls expressed a comparable amount of the human E domain mRNA in muscle and liver, which was absent in the ERαKO and wild-type (WT) (Supplementary Fig. 1*D*). NOER mice genotyping confirmed the presence of the knockin mutation at position 451 of the ERα gene (Supplementary Fig. 1*C*). WT littermates were used as controls; if not available, C57BL/6N mice (Charles River Laboratories) were used as controls. All experiments were approved by the Institutional Animal Care and Use Committee of Tulane University in accordance with National Institutes of Health guidelines. Mice were studied between the ages of 5 and 12 months.

### Metabolic Studies and Hormone Measurements

Random-fed blood glucose and plasma insulin levels were measured in the morning (3–4 h after the beginning of the light cycle). Fasting blood glucose and plasma insulin levels were measured after 16 h of fasting (overnight). A glucose tolerance test (GTT), glucose-stimulated insulin secretion (GSIS) test, and pyruvate tolerance test (PTT) were performed after 16 h of fasting. An insulin tolerance test (ITT) was performed after 6 h of fasting. Mice were injected i.p. with glucose for GTT (2 g/kg) and GSIS (3 g/kg), sodium pyruvate for PTT (2 g/kg), or insulin for ITT (0.5–0.75 units/kg for females, 0.75–1.25 units/kg for males). The brain glucose-sensing experiment was performed as described previously (24,25) after right carotid catheterization and the injection of a bolus of glucose (25 mg/kg). Blood was sampled from the tail vein at indicated times for glucose and/or insulin assessment. Blood glucose was measured using the True Result Glucose Meter (Nipro Diagnostics). Plasma insulin levels were measured by ELISA (Millipore). At sacrifice, blood was sampled from the inferior vena cava and serum was collected for measurement of testosterone (IBL America), luteinizing hormone (LSBio), E2 (Calbiotech), and interleukin-6 (IL-6) (R&D Systems) by ELISA. Nonesterified fatty acids (Cell Biolabs, Inc.) were measured from EDTA-treated plasma after a 16 h of fasting.

### Hyperinsulinemic-Euglycemic Clamp

Whole-body glucose turnover ($G_t$) was quantified using a hyperinsulinemic-euglycemic clamp with isotope tracer. Under isoflurane anesthesia, female MOER mice were catheterized with a silastic catheter into the jugular, with the other end tunneled out the neck skin. Postrecovery, mice were fasted for 6 h in a cage where they were freely moving. For some mice, a basal glucose level was ascertained by perfusing saline containing high-performance liquid chromatography–purified 3-$^3$H D-glucose (0.05 μCi/min; ARC) for 2 h before the beginning of the clamp. A continuous infusion of insulin (4 mU/kg/min) (Humulin; Lilly) was started to induce hyperinsulinemia. The insulin solution contained glucose tracer (0.1 μCi/min; ARC) to measure the $G_t$ (4-μL bolus in 1 min, then a constant rate of 1 μL/min for 120 min). A variable glucose infusion rate (GIR) of a 15% D-glucose solution was adjusted to maintain blood glucose concentration at ~100 mg/dL. Blood glucose was measured every 20 min from the tail vein (no restraint). Blood samples were collected at $t$ = 100, 110, and 120 min to assess glucose-specific activity. Blood was deproteinized with $ZnSO_4$ and $Ba(OH)_2$, and the supernatant was dried to remove $^3H_2O$, resuspended in water, and counted in scintillation fluid (Ultima Gold; PerkinElmer) with a β-counter (Packard; Tulane University Shared Instrument Facility). Whole-body $G_t$ (in milligrams per kilogram per minute) was determined as the ratio of the 3-$^3$H GIR (desintegration per minute/kg/min) to the specific activity of blood glucose (desintegration per minute/mg) during the final 20 min of clamp. Endogenous glucose production (EndoRa) was calculated as EndoRa = $G_t$ − GIR. Plasma insulin concentration was determined from blood samples at $t$ = 0 and $t$ = 120 min. At the end of the 120-min period, mice were anesthetized and tissues were collected and snap frozen in liquid nitrogen.

### Central Glucose-Induced Insulin Secretion

In order to test in vivo the ability of the central nervous system to induce insulin secretion in response to glucose (glucose sensing), male mice were injected with glucose into the brain, as described previously (24). Briefly, a catheter was introduced into the carotid artery under anesthesia (200 mg/kg; Inactin). A bolus of glucose (30 μL, 25 mg/kg) was injected into the brain. This dose was not sufficient to alter peripheral blood glucose concentration. Blood samples

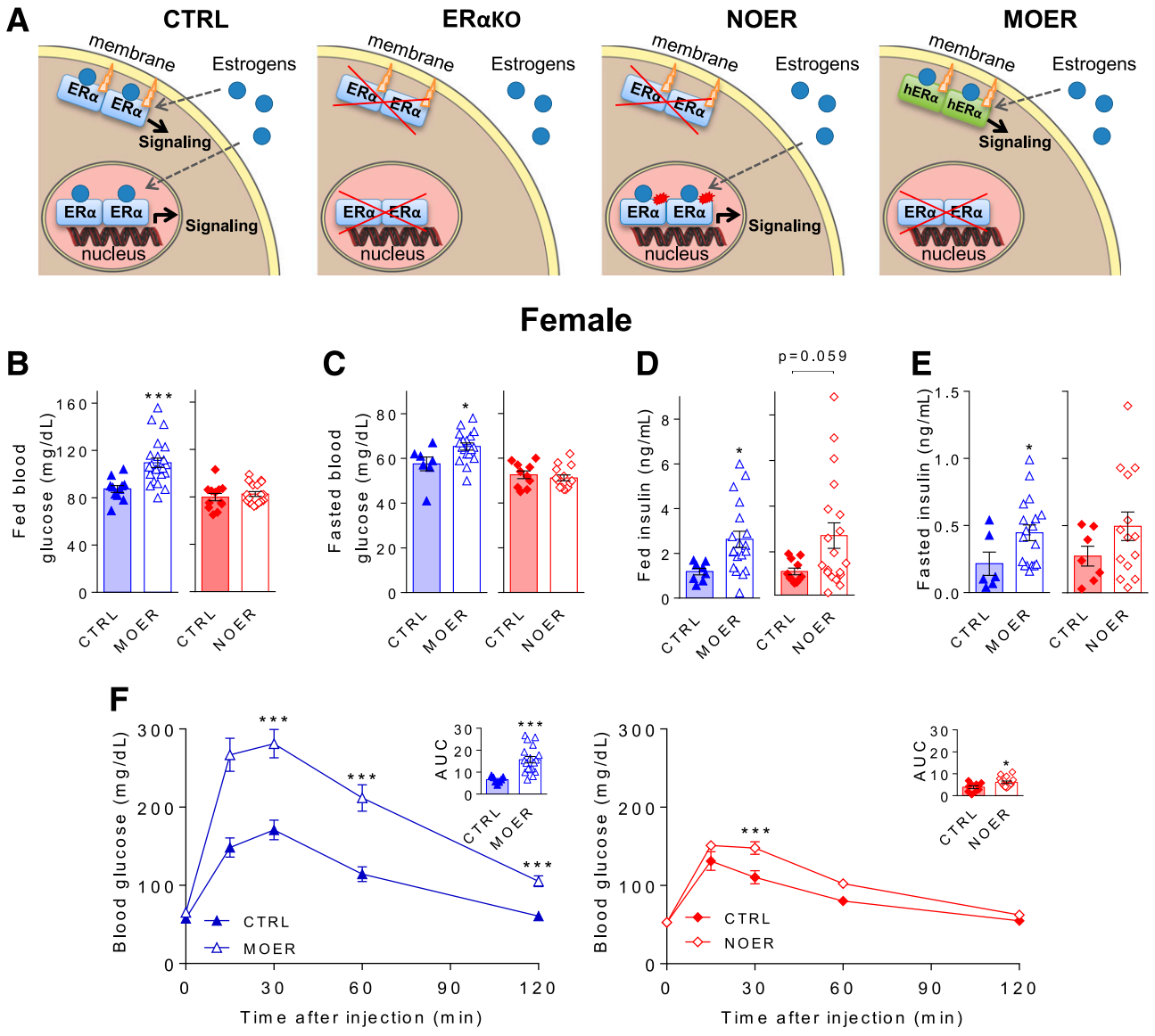


**Figure 1**—Female MOER mice are hyperglycemic and glucose intolerant. *A*: The control (CTRL) mice express NOER and MOER. Global ERαKO mice lack ERα. NOER mice exhibit a mutation of the ERα palmitoylation site, leading to exclusive ERα nuclear location. MOER mice are ERαKO mice re-expressing the human ERα ligand-binding domain selectively at the membrane. Random-fed (*B*) and fasting blood glucose (*C*), random-fed (*D*) and fasting plasma insulin (*E*) levels, and blood glucose and calculated area under the curve (AUC, inset) (*F*) during a GTT (i.p. GTT, 2 g/kg) in 6-month-old female MOER and NOER mice with their respective CTRL littermates. Data correspond to the mean ± SEM ($n$ = 6–23). *$P < 0.05$, ***$P < 0.001$.

were collected from the tail vein 0, 1, 3, and 5 min post-injection to measure blood glucose and plasma insulin levels.

### Central Insulin Perfusion

The central infusion of insulin was performed as described previously (26). Briefly, a single cannula guide (Plastics One) was inserted into the lateral ventricle. After recovery and 16 h of fasting, mice were perfused intracerebroventricularly with insulin (10 μU/μL, 1 μL in a 1-min bolus then 1 μL/h) (UltraMicroPump III, WPI; Humulin, Lilly) or vehicle (artificial cerebrospinal fluid). After 3 h, mice were euthanized, tissues were dissected, and snap frozen for further analysis.

### Insulin Secretion in Static Incubation

After islet isolation via pancreatic duct cannulation, experiments of static incubation were performed as described previously (21). Insulin secretion was expressed as a percentage of total insulin content.

### Immunohistochemistry and β-Cell Mass Measurement

Pancreata were dissected, weighed, and fixed in 10% neutral buffered formalin before paraffin embedding. Pancreas sections (5 μm) were prepared by the Tulane University Stem Cell Research and Regenerative Medicine Histology Laboratory. Sections were dewaxed and rehydrated before antigen demasking using citrate buffer. After

permeabilization, slides were incubated with guinea pig anti-insulin antibody (Linco or Abcam) and donkey anti-guinea pig Cy3 antibody (The Jackson Laboratory). Nuclei were counterstained using DAPI. Each islet and the entire pancreas were photographed using a Nikon Eclipse Ti and Olympus microscope, respectively (Tulane University Center of Biomedical Research Excellence Molecular Core). Individual pancreas pictures were reconstituted using the stitching function of the Metamorph Software (Nikon). Insulin-positive areas were quantified using ImageJ software. The β-cell mass (in milligrams) was calculated by morphometric analysis by multiplying the β-cell area (insulin-positive area/entire pancreas area; %) by the mass of the entire pancreas.

### Western Blotting

Tissues were homogenized in radioimmunoprecipitation assay buffer containing antiphosphatases and antiproteases cocktails (Roche), and protein concentration was determined using the Pierce BCA Protein Assay Kit (Thermo Fisher Scientific). Thirty to 50 μg of protein was separated by electrophoresis using 10% or 12% premade SDS-PAGE gels (BIO-RAD) then transferred to nitrocellulose membranes (Invitrogen). Membranes were incubated with the indicated antibodies (pAkt S473, pAKT T308, Akt, pSTAT3 Y705, STAT3; Cell Signaling Technology), followed by incubation with fluorophore-coupled anti-rabbit IgG (LI-COR) or horseradish peroxidase–linked anti-rabbit IgG (Santa Cruz Biotechnology). The fluorescent signal was acquired using the Odyssey Imaging System (LI-COR) or the ChemiDoc MP Imaging System (BIO-RAD). Band density quantification was performed using ImageJ or Image Lab Software (BIO-RAD).

### Real-time Quantitative PCR

RNA was extracted from the liver using TRIzol reagent (Thermo Fisher Scientific) following manufacturer instructions. cDNA synthesis (1 μg) was performed using the iScript cDNA Synthesis Kit (BIO-RAD). PCRs were prepared using iQ SYBR Green Supermix (BIO-RAD), and PCRs were performed in a LightCycler 96 Instrument real-time detection system (Roche LifeScience). Quantification of a given gene (IL-6; primer sequences are available upon request), expressed as the relative mRNA level compared with control, was calculated with the 2-ddCT comparative method after normalization to the β-actin housekeeping gene.

### Statistics

Statistical analyses were performed with GraphPad Prism. Normality of the samples was checked using the Kolmogorov-Smirnov test. When the samples assumed a Gaussian distribution, a Student *t* test or a one-way ANOVA (with Bonferroni post hoc test) were performed when appropriate. Otherwise, the Mann-Whitney or Kruskal-Wallis test was used. Results are expressed as the mean ± SEM, and $P < 0.05$ was considered to be significant. Significance is expressed as follows: $^{*}P < 0.05$, $^{**}P < 0.01$, $^{***}P < 0.001$.

## RESULTS

### Loss of Nuclear ERα, and to a Lesser Extent Membrane ERα, Impairs Glucose Homeostasis in Mice of Both Sexes

To determine the relative contributions of NOER and MOER pools to glucose homeostasis, we studied NOER and MOER male and female mice. ERαKO mice were initially used as controls of global ERα deficiency (Fig. 1*A*). Female MOER mice exhibited fed and fasted hyperglycemia (Fig. 1*B* and *C*) and hyperinsulinemia (Fig. 1*E* and *D*) to an extent similar to that of ERαKO mice (Supplementary Fig. 2*A*). Female NOER mice exhibited fed and fasted blood glucose levels comparable to those of littermate WT controls (Fig. 1*B* and *C*), even though their fasting and fed plasma insulin levels were nonsignificantly increased, suggesting insulin resistance (Fig. 1*E* and *D*). After an i.p. GTT, female MOER mice, and to a lesser extent NOER mice, exhibited glucose intolerance, as observed in ERαKO mice (Supplementary Fig. 2*B*), compared with the littermate controls (Fig. 1*F*).

Like females, male MOER mice exhibited fed and fasted hyperglycemia (Fig. 2*A* and *B*) similar to ERαKO mice (Supplementary Fig. 2*C*), whereas male NOER mice remained normoglycemic (Fig. 2*A* and *B*). However, unlike in the case of females, plasma insulin levels of male MOER and NOER mice were not significantly different from those of littermate controls, suggesting that they were not insulin resistant (Fig. 2*C* and *D*). Only fasting plasma insulin levels were elevated in male MOER mice (Fig. 2*C* and *D*) and showed a trend toward elevation in ERαKO (Supplementary Fig. 2*C*). After an i.p. glucose challenge, male MOER and ERαKO mice, but not NOER mice, exhibited glucose intolerance (at 2 h into the GTT) compared with their littermate controls (Fig. 2*E* and Supplementary Fig. 2*D*). Male NOER mice also responded normally to an oral glucose challenge (Supplementary Fig. 3).

These results suggest that nuclear ERα is essential for maintaining glucose homeostasis in male and female mice but suggests that sex-specific mechanisms are involved.

### Loss of NOER and MOER Produces Hepatic Insulin Resistance in Female Mice

We assessed insulin sensitivity in physiological conditions via ITT in male and female MOER and NOER mice. Female MOER mice, like ERαKO mice, exhibited resistance to the hypoglycemic effect of insulin, as demonstrated by a smaller decrease in blood glucose level after insulin injection compared with their controls, whereas female NOER mice exhibited normal insulin sensitivity (Fig. 3*A* and Supplementary Fig. 4*A*). In contrast, during the ITT, male MOER mice exhibited normal insulin sensitivity that was comparable to that of male NOER and ERαKO mice (Fig. 3*B* and Supplementary Fig. 4*B*). Both female and male MOER mice showed a similar increase in subcutaneous

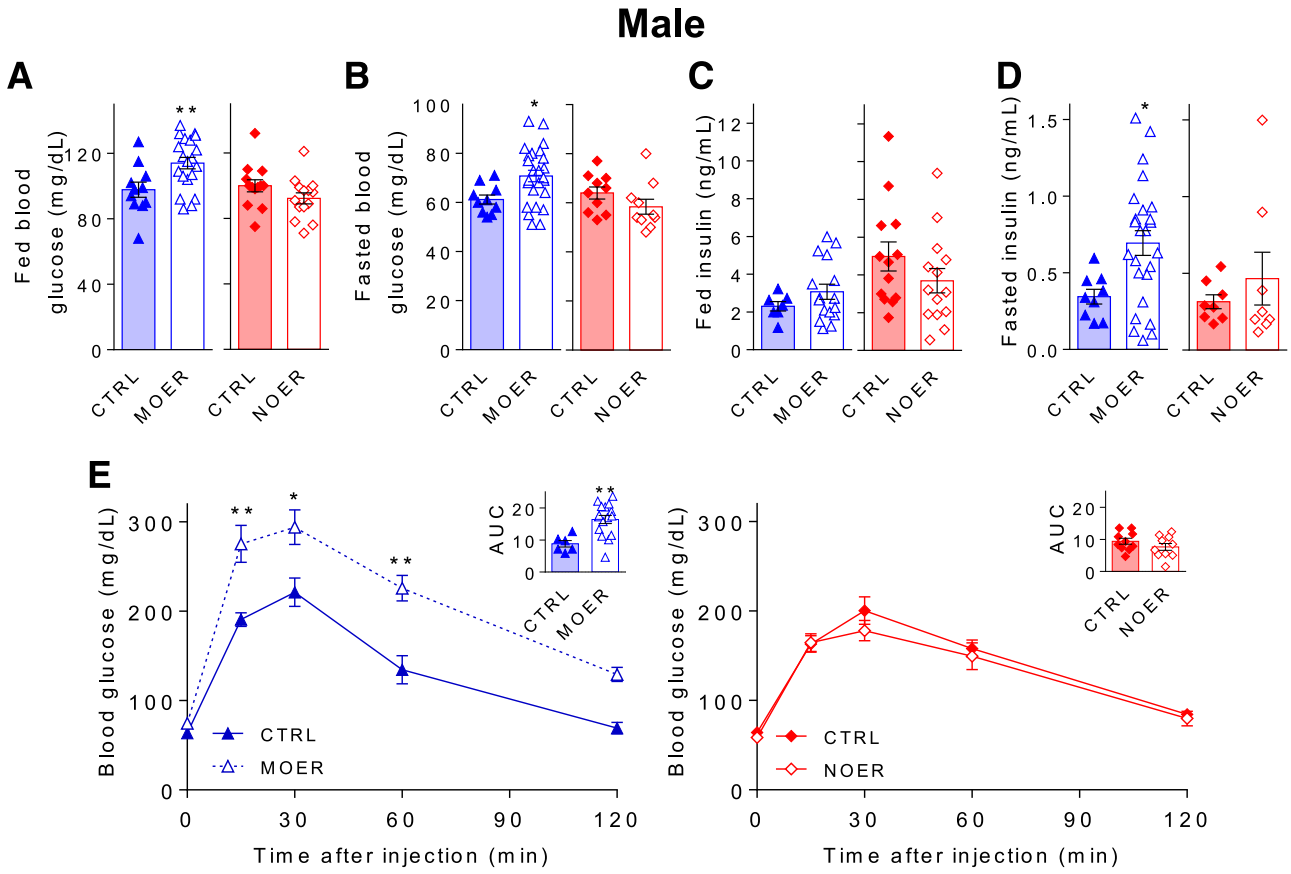


**Figure 2**—Male MOER mice are hyperglycemic and glucose intolerant. Random-fed (*A*) and fasting blood glucose (*B*), random-fed (*C*) and fasting plasma insulin (*D*) levels, and blood glucose and calculated area under the curve (AUC, inset) (*E*) during a GTT (i.p. GTT, 2 g/kg) in 6-month-old male MOER and NOER mice with their respective control (CTRL) littermates. Data correspond to the mean ± SEM ($n$ = 6–25). $^*P < 0.05$, $^{**}P < 0.01$. AUC, area under the curve.

inguinal, mesenteric, and perigonadal adipose tissues compared with control mice, which was not observed in NOER mice (Fig. 3*C*–*F*), eliminating a potential role for adiposity in the insulin resistance observed in female MOER mice compared with male MOER mice. Note that male MOER mice showed an increase in fat mass without a significant increase in body weight, likely due to the deleterious effect of ERα deletion on lean mass in the male (27,28).

Having observed that female MOER mice are hyperinsulinemic and insulin resistant during ITT and that female NOER mice exhibit a nonsignificant fasting and fed hyperinsulinemia, suggesting insulin resistance (not detected during the ITT), we explored systemic insulin sensitivity during a hyperinsulinemic-euglycemic clamp in female MOER and NOER mice. During the clamp, we increased plasma insulin levels by a factor of 3–6 from fasted levels in MOER and NOER mice and littermate controls (Supplementary Fig 5*A* and *D*). Blood glucose levels were maintained to similar levels in MOER and NOER mice and their littermate controls (Supplementary Fig. 5*B* and *E*), with no difference in blood glucose levels at the end of the 2 h (Supplementary Fig. 5C and *F*) by adjusting the GIR. The GIR was decreased in female MOER (Fig. 4*A*) and NOER (Fig. 4*D*) mice compared with littermate control mice, demonstrating systemic insulin resistance. Based on tracer-specific activity determination at the end of the clamp, there was no difference in insulin-stimulated whole-body $G_t$ between female control and littermate MOER and NOER mice (Fig. 4*B* and *E*). However, the endogenous glucose production (EndoRa) was more elevated in the female MOER mice (Fig. 4*C*) and to a lesser extent in NOER mice (Fig. 4*F*) compared with control mice, suggesting hepatic insulin resistance. We explored the mechanism of insulin resistance in female MOER mice only. To explore liver gluconeogenesis, we examined pyruvate incorporation into glucose via gluconeogenesis after a PTT. After pyruvate injection, in agreement with the EndoRa (Fig. 4*C*), female MOER mice exhibited higher blood glucose levels, which did not return to basal level by 2 h postinjection (Fig. 4*G*). Together, these data suggest that female MOER mice exhibit insulin resistance via increased hepatic glucose output from unsuppressed gluconeogenesis. Direct insulin signaling, as assessed by insulin-stimulated Akt phosphorylation on Ser 473 and Thr 308 in liver (Fig. 4*H*) and skeletal muscle (Supplementary Fig. 6) isolated from clamped MOER mice,

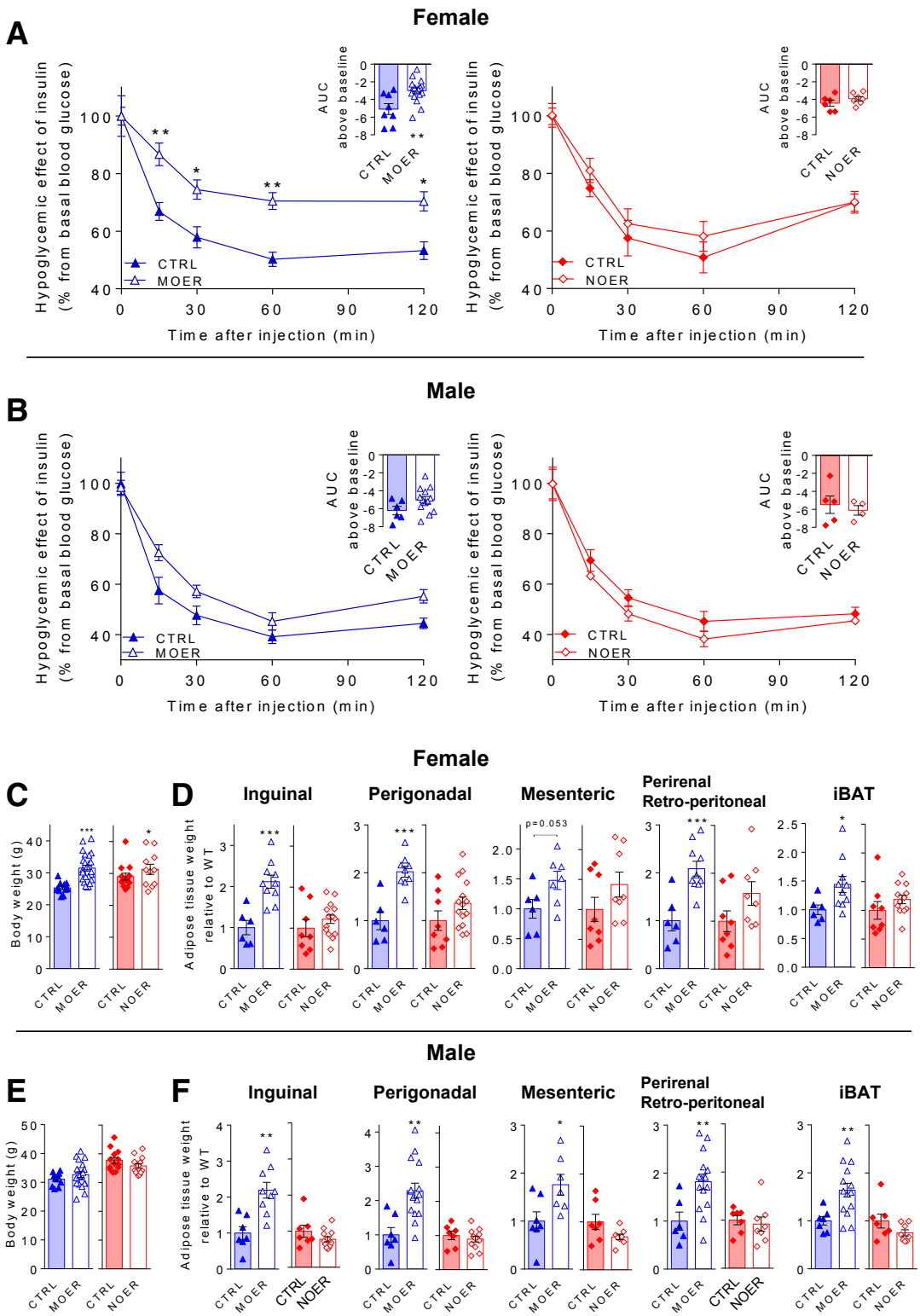


**Figure 3—**Female MOER mice exhibit hepatic insulin resistance. Blood glucose level during an ITT (i.p. ITT) in 6-month-old female mice (0.5–0.75 units/kg) (*A*) and male (0.75–1.25 units/kg) MOER and NOER mice (*B*) with their respective control (CTRL) littermates. Data correspond to the mean ± SEM ($n$ = 4–19). Body weight of 6-month-old female (*C*) and male (*E*) NOER and MOER mice with their respective control (CTRL) littermates. Adipose tissue weight in the indicated fat pads of 6-month-old female (*D*) and male (*F*) NOER and MOER mice with their respective CTRL littermates. Data correspond to the mean ± SEM ($n$ = 6–24). AUC, area under the curve; iBAT, inguinal brown adipose tissue. $^{*}P < 0.05$, $^{**}P < 0.01$, $^{***}P < 0.001$.

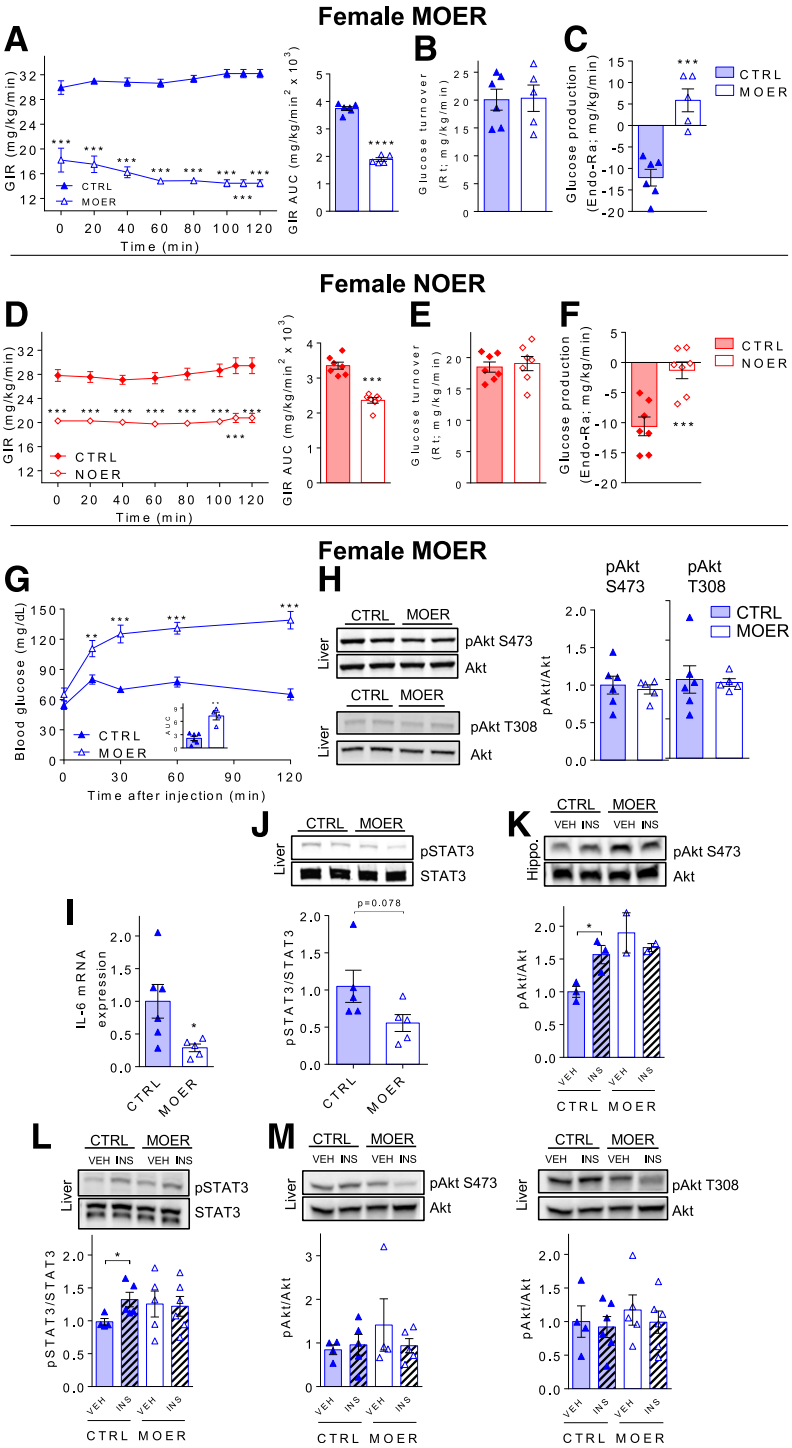


**Figure 4—**Female MOER mice exhibit central insulin resistance. GIR (left panel) and corresponding area under the curve (AUC) (right panel) calculated during a hyperinsulinemic-euglycemic clamp in female control (CTRL) and MOER mice (*A*) and female CTRL and NOER mice (*D*). Glucose turnover (Rt, mg/kg/min) in CTRL and MOER (*B*) and CTRL and NOER (*E*) female mice. EndoRa (in mg/kg/min) in female CTRL and MOER (C) and CTRL and NOER (*F*) mice. Clamp was performed in 6-month-old mice ($n$ = 5–6). *G*: Blood glucose and calculated AUC (inset) during a PTT (i.p. PTT, 2 g/kg) in female CTRL and MOER mice ($n$ = 4–6). *H*: Protein expression for pAkt (S473), pAkt (T308), and total Akt in liver from female MOER mice at the end of the 2-h clamp were analyzed by Western blotting. Quantification by densitometry is shown in adjacent bar graphs ($n$ = 5–6). *I*: Hepatic IL-6 mRNA expression quantified by quantitative PCR in female mice at the end of the 2-h clamp ($n$ = 5–6). *J*: Protein expression for pSTAT3 (Y701) and STAT3 in liver from female MOER mice at the end of the 2-h clamp were analyzed as in *H*. *K*: Protein expression for pAkt (S473)/Akt in hippocampus from female CTRL and MOER at the end of 3 h of intracerebroventricular perfusion of vehicle (VEH) or insulin (INS). Quantification by densitometry is shown in adjacent bar graphs ($n$ = 2–3). Protein expression for pSTAT3/STAT3 (*L*) and pAkt (S473)/Akt and pAkt (T308)/Akt (*M*) in liver from female CTRL and MOER mice at the end of 3 h of intracerebroventricular perfusion of vehicle or insulin analyzed as in *L* ($n$ = 4–6). Data correspond to mean values ± SEM. *$P < 0.05$, **$P < 0.01$, ***$P < 0.001$, ****$P <$ 0.0001.

was unchanged compared with that of controls, suggesting that insulin resistance is mediated via extrahepatic tissues and/or other signaling pathways.

### Loss of Nuclear ERα Alters the Central Control of Insulin Sensitivity in Female Mice

Central insulin is known to suppress hepatic glucose production (HGP) via the autonomic nervous system and a liver IL-6-STAT3 axis (26,29). In liver isolated from hyperinsulinemic clamped MOER mice, IL-6 mRNA expression was decreased compared with controls (Fig. 4*I*) without changes in IL-6 serum concentrations (mean ± SEM: controls 3.78 ± 1.1 pg/mL; MOER mice 4.46 ± 0.6 pg/mL). Additionally, STAT3 phosphorylation (Fig. 4*J*) was also decreased compared with controls, together suggesting a reduced ability of central insulin to lower HGP.

To assess the ability of brain insulin to activate the hepatic IL-6-STAT3 pathway and suppress HGP in female MOER mice, we performed intracerebroventricular insulin injection. We used the hippocampus as a control, insulin-sensitive brain region known to develop insulin resistance under diabetic conditions (30). Accordingly, the injection of insulin into the lateral ventricle increased hippocampal Akt phosphorylation in control mice (Fig. 4*K*). However, intracerebroventricular insulin perfusion produced no increase in hippocampal Akt phosphorylation in female MOER mice, which is consistent with central insulin resistance (Fig. 4*K*). As described previously (29), intracerebroventricular perfusion of insulin stimulated the hepatic phosphorylation of STAT3, without canonical phosphorylation of Akt in control mice (Fig. 4*L* and *M*). However, unlike in controls, the intracerebroventricular insulin perfusion did not stimulate hepatic STAT3 phosphorylation in female MOER mice (Fig. 4*L*). Thus, female MOER mice exhibit central insulin resistance associated with decreased liver IL-6-STAT3 activation and increased HGP.

### Loss of Nuclear ERα Alters the Central Control of Insulin Secretion in Male Mice

Male MOER mice exhibited fasting and fed hyperglycemia and glucose intolerance without alteration in insulin sensitivity during ITT, suggesting that these mice might have altered insulin secretion. We assessed GSIS in vivo after an i.p. glucose challenge in male MOER mice. Although control mice exhibited a fourfold increase in first-phase insulin release after glucose injection, the first-phase insulin release was blunted in male MOER mice (Fig. 5*A*), as observed in male ERαKO mice (Supplementary Fig. 7). Male MOER mice exhibited no alteration in β-cell mass (Fig. 5*B*) or pancreas insulin content (Fig. 5*C*), suggesting a functional defect of the β-cells in these mice. In contrast to the decreased acute phase insulin secretion, plasma insulin levels 30 min post–glucose injection (which represents the second phase of insulin secretion) were increased in male MOER mice (Fig. 5*D*). To determine whether the defect in GSIS observed in male MOER mice was islet cell autonomous, we performed GSIS in static incubation from cultured isolated islets from male MOER mice. Unlike what was observed in vivo, GSIS and islet insulin content were identical in cultured male MOER and control islets in the presence or absence of E2 (Fig. 5*E–H*). This suggests that the defect in acute-phase insulin release observed in MOER mice results from an extraislet factor. Unlike males, female MOER and NOER mice exhibited no defect in acute-phase insulin release during GSIS and, accordingly, no defect in β-cell mass and or pancreas insulin content (Fig. 5*K–M* and Supplementary Fig. 8*A–C*). However, consistent with the insulin resistance described above, plasma insulin levels 30 min post–glucose injections were increased in female MOER and NOER mice (Fig. 5*N* and Supplementary Fig. 8*D*). Therefore, MOER mice exhibit a male-specific defect in acute insulin release in vivo.

To search for an extraislet factor altering GSIS selectively in male MOER, we first studied estrogen and androgen concentrations (31). Female MOER mice exhibited a fivefold increase in circulating E2 concentrations and a 10-fold increase in circulating testosterone concentrations compared with levels observed in littermate control males (Table 1, Male CTRL). The testosterone/E2 ratio was increased twofold in female MOER mice. Male MOER mice did not show any differences in E2 levels but exhibited a threefold increase in testosterone concentrations compared with controls (Table 1). As a result, male MOER mice exhibited a threefold increase in the testosterone/E2 ratio. To assess the potential role of increased testosterone in the altered in vivo GSIS of males, we treated male MOER mice with the androgen receptor antagonist flutamide. Flutamide was efficient in producing androgen resistance as assessed by increased testosterone concentrations, but produced no improvement in GSIS in male mice, ruling out the role of excess testosterone (Supplementary Fig. 9).

The central nervous system modulates insulin secretion in vivo, via a hypothalamo-pancreatic axis (32). To assess the extent to which brain glucose sensing was altered in male MOER mice, we performed a gold standard experiment to assess central GSIS by glucose injection in the carotid artery (24,25). As previously reported, the carotid glucose bolus did not affect peripheral glucose levels in control and MOER mice (Fig. 5*I*). In male control mice, glucose injection triggered an acute insulin secretion 1 min post–glucose injection (Fig. 5*J*). In contrast, in male MOER mice, the acute insulin secretion was blunted (Fig. 5*J*). Thus, the nuclear ERα is necessary to maintain GSIS in male mice, and this is at least partially dependent on brain-induced GSIS.

## DISCUSSION

Loss of nuclear ERα differentially impairs glucose homeostasis in male and female mice being fed a normal chow diet. Although insulin resistance is predominant in female mice, impaired GSIS is central in males.

Female MOER mice, lacking nuclear ERα, are hyperinsulinemic and insulin resistant during the physiological conditions of an insulin challenge. Under these conditions,

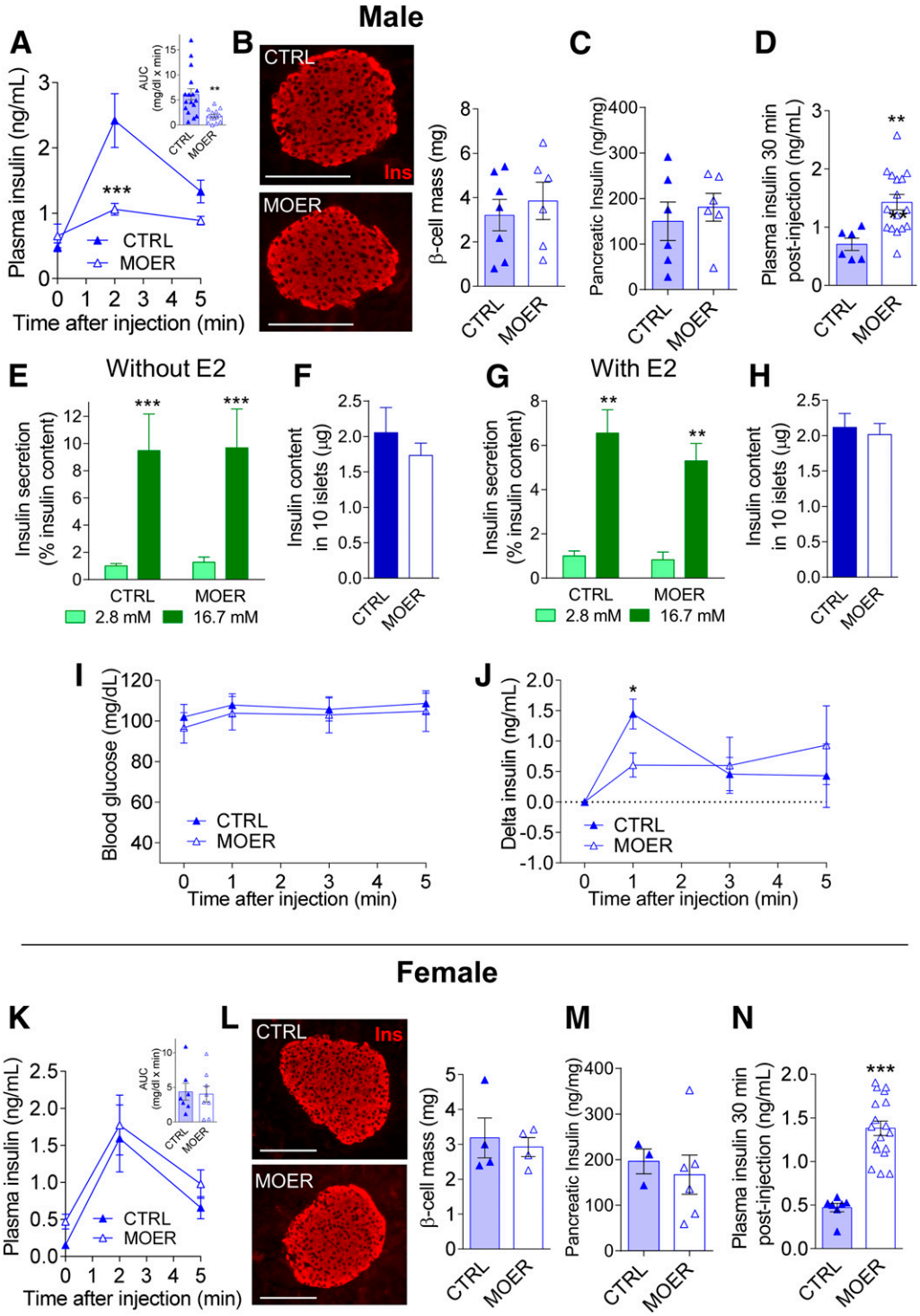


**Figure 5—**Male MOER mice exhibit reduced first-phase insulin secretion in vivo. *A*: Plasma insulin (left panel) and calculated area under the curve (AUC) (right panel) during an in vivo i.p. GSIS test (GSIS, 3 g/kg) in male control (CTRL) and MOER mice ($n$ = 14–17). *B*: Representative pictures of pancreatic islets stained for insulin (red) and calculated β-cell mass (mg, $n$ = 6–7) in mice from *A*. Scale bar, 100 μm. *C*: Pancreatic insulin content in male CTRL and MOER mice ($n$ = 6). *D*: Plasma insulin levels 30 min after an i.p. injection of glucose (2 g/kg), showing the second-phase insulin secretion in male CTRL and MOER mice ($n$ = 6–16). In vitro GSIS in static incubation in cultured islets isolated from MOER and CTRL male mice without E2 (*E*) or with E2 (*G*) ($10^{-8}$ mol/L). *F* and *H*: Insulin content of islets from *E* and *G* ($n$ = 8–19 islet batches from three to seven different animals). Blood glucose (*I*) and plasma insulin (*J*) levels during a brain glucose-sensing test (25 mg/kg glucose) in male CTRL and MOER ($n$ = 10–11, five independent experiments). *K*: Plasma insulin (left panel) and calculated AUC (right panel) during an in vivo GSIS (3 g/kg) in female CTRL and MOER mice ($n$ = 7–8). *L*: Representative pictures of female CTRL and MOER pancreatic islets stained for insulin (red) and calculated β-cell mass (in mg; $n$ = 4). Scale bar, 100 μm. *M*: Pancreatic insulin content in female CTRL and MOER mice ($n$ = 3–7). *N*: Plasma insulin levels 30 min after an i.p. injection of glucose (2 g/kg), showing the second phase of insulin secretion in female CTRL and MOER mice ($n$ = 7–18). Data were collected from 6- to 8-month-old mice and correspond to mean values ± SEM. $^{*}P < 0.05$, $^{**}P < 0.01$, $^{***}P < 0.001$.

**Table 1—Metabolic parameters in control and MOER mice**

| | LH (ng/mL) | E2 (pg/mL) | Testosterone (ng/mL) | Testosterone/E2 ratio (pg/mL) |
|---|---|---|---|---|
| Female CTRL | 2.5 ± 0.5 | 4.2 ± 0.4 | 0.2 ± 0.03 | 44.5 ± 6.8 |
| Female MOER | 1.2 ± 0.2 | 22.6 ± 5.5* | 1.9 ± 0.5** | 84.7 ± 17.1 |
| Male CTRL | 7.4 ± 2.1 | 4.5 ± 0.2 | 1.3 ± 0.2 | 261.0 ± 40.2 |
| Male MOER | 4.6 ± 1.5 | 3.9 ± 0.2 | 3.5 ± 1.0** | 892.0 ± 257.1** |

Serum luteinizing hormone (LH), E2, testosterone, and testosterone/E2 ratio were measured in 6-month-old MOER and control (CTRL) mice. Data correspond to the mean ± SEM ($n$ = 4–6). *$P < 0.05$; **$P < 0.01$.

female NOER mice, lacking membrane ERα, are only slightly hyperinsulinemic. However, both MOER and, to a lesser extent, NOER mice show systemic insulin resistance during the steady-state conditions of a hyperinsulinemic-euglycemic clamp. Thus, both NOER and MOER are involved in insulin sensitivity in female mice, with the nuclear pool of ERα playing a predominant role.

Female mice with global (6,33) or liver-specific knockout of ERα (LERKO) (5,34) exhibit a decline in the ability of insulin to suppress HGP during hyperinsulinemic-euglycemic clamp studies, suggesting that ERα in hepatocytes is important to whole-body and liver insulin sensitivity in female mice. Additionally, conditional elimination of ERα in skeletal muscle promotes systemic insulin resistance and secondary failure of insulin to suppress HGP in female mice (7). Female MOER mice exhibit hepatic insulin resistance (increased EndoRa and hepatic gluconeogenesis) without detectable abnormality in muscle insulin action as assessed by whole-body $G_t$ (and insulin stimulation of Akt phosphorylation in muscle). Thus, the primary site of systemic insulin resistance in female MOER mice seems to be the liver. Loss of hepatocyte NOER (5,34) or increased testosterone action in hepatocytes (35) could promote liver insulin resistance in female MOER mice. However, unlike female LERKO mice or female mice with excess testosterone fed a high-fat diet, when fed a normal chow diet female MOER mice do not exhibit insulin failure to promote Akt phosphorylation. Thus, the defect leading to unsuppressed HGP in female MOER mice seems to originate outside the liver.

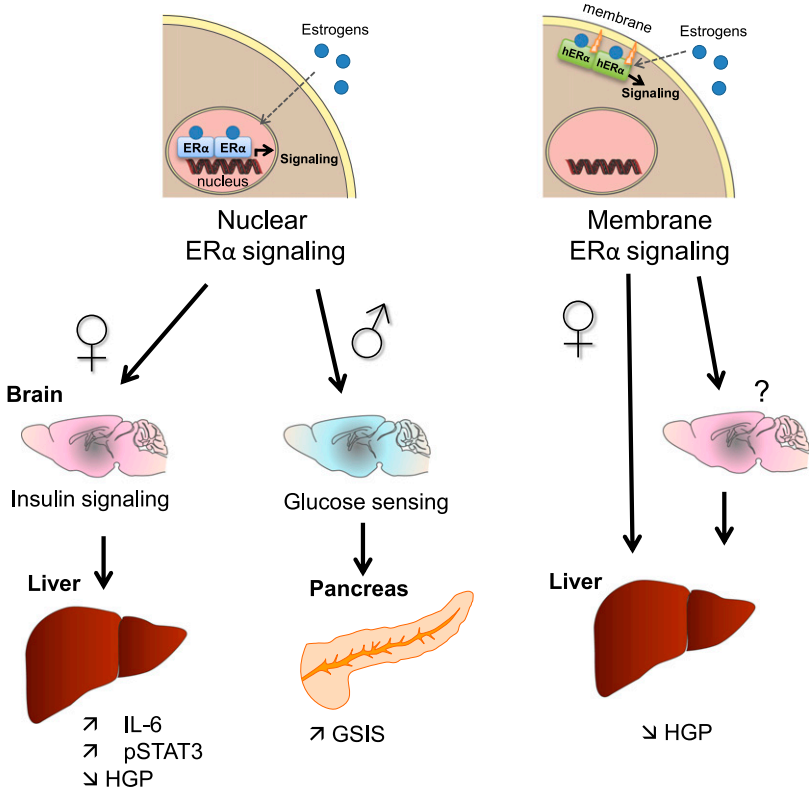


**Figure 6**—Sex differences in NOER and MOER effects on glucose homeostasis. In female mice, NOER signaling in the brain promotes the suppression of HGP via a brain-liver IL-6-STAT3 axis. MOER also participates in control of HGP. In male mice, NOER action in the brain favors glucose-stimulated first-phase insulin secretion.

Hypothalamic insulin action suppresses HGP in mice (36). Central insulin blunts parasympathetic output to Kupffer cells, increasing their production of IL-6 leading to the activation of STAT3 in nearby hepatocytes, which downregulates gluconeogenic genes (26,29). Female MOER mice exhibit central insulin resistance with the failure of central insulin infusion to activate Akt in the hippocampus. Further, female MOER mice exhibit decreased hepatic IL-6-STAT3 activation during hyperinsulinemic clamp and central insulin infusion. Taken together, these results suggest that global nuclear ERα deficiency impairs central insulin action and the activation of the hepatic IL-6-STAT3 pathway, leading to inappropriate suppression of HGP. Inhibitory insulin action in Agouti-related protein (AgRP) neurons of the arcuate nucleus of the hypothalamus (ARC) is required to suppress HGP via the brain-liver IL-6 pathway (36,37). However, ERα is not expressed in mouse AgRP neurons (38). Rather, ERα is expressed in proopiomelanocortin (POMC) neurons, and female mice lacking ERα specifically in POMC neurons exhibit insulin resistance when fed a chow diet, like female MOER mice (39). Moreover, E2 enhances insulin action in POMC neurons by stimulating their neuronal excitability and the coupling of insulin receptors to TRPC5 channels via transcriptional mechanisms (40). Therefore, in female mice, the loss of ERα transcriptional activity in POMC neurons is likely to decrease neuronal excitability and the inhibition of AgRP neurons, which could increase HGP.

Global loss of NOER in female MOER mice promotes central insulin resistance, leading to unsuppressed HGP. In contrast, hepatocyte-specific knockout of ERα in LERKO mice promotes peripheral insulin resistance via impairment of Akt in hepatocytes. One explanation for this apparent discrepancy is likely related to differences in diets and models. Female MOER mice were fed normal chow, and in these conditions the neuronal ERα seems predominant in suppressing HGP in mice (via liver IL-6-STAT3 and without activation of hepatocytes Akt). In contrast, female mice LERKO were fed a high-fat diet. Given the importance of hepatocyte ERα in limiting liver fat accumulation, during high-fat feeding insulin resistance in hepatocytes via Akt (5,34) is predominant.

Male MOER mice, lacking nuclear ERα, exhibit mild fasting hyperinsulinemia but no detectable insulin resistance. Male NOER mice, lacking membrane ERα, have no detectable abnormalities of glucose homeostasis. Male MOER mice exhibit blunted first-phase insulin release in response to glucose in vivo. The first-phase insulin release is central to glucose homeostasis in mice (41,42), and impaired first-phase GSIS with exaggerated second-phase GSIS is a hallmark of the early stages of type 2 diabetes (43). Therefore, loss of NOER in male mice produces a defect that is typical of human type 2 diabetes. The GSIS defect of male MOER mice is not observed in cultured islets, demonstrating that it is independent from the loss of NOER in β-cells and secondary to the loss of ERα in extraislet tissues, indirectly impairing islet function possibly via a neural factor. To assess the role of nuclear ERα in β-cell function via the hypothalamo-pancreatic axis, we studied acute insulin release in response to the central injection of glucose. We observed that brain glucose sensing was impaired in male MOER mice with a blunted acute insulin response to a bolus of glucose directed toward the brain, suggesting that the response to central glucose and the neural control of insulin secretion are impaired by the loss of NOER in male mice. Efferent circuits that emanate from the hypothalamus innervate pancreatic islets, and glucose sensing in the ARC is important to GSIS in male mice (32). Therefore, loss of NOER transcriptional activity in ARC neurons may impair parasympathetic outflow to the islets.

In summary, the global lack of NOER and, to a lesser extent, MOER alter the central control of HGP in female mice (Fig. 6). In male mice, THE lack of NOER predominantly impairs the central regulation of insulin secretion (Fig. 6). Further studies are needed to identify the neuronal population mediating these sexually dimorphic effects of ERα on glucose homeostasis.

**Funding.** This work was supported by grants from the National Institutes of Health (NIH) (R01-DK-074970 and DK-107444) and a U.S. Department of Veterans Affairs Merit Review Award (BX003725) to F.M.-J. C.A. was supported by American Diabetes Association Post-Doctoral Fellowship (1-16-PDF-004). A.Z. was supported by NIH R01-DK-099598.

**Duality of Interest.** No potential conflicts of interest relevant to this article were reported.

**Author Contributions.** C.A. designed and performed experiments, analyzed the data, and wrote the manuscript. J.J.M. performed experiments, analyzed the data, and revised the manuscript. B.X., B.S., W.X., and L.D. performed experiments. A.Z. revised the manuscript. J.K.K. and E.R.L. discussed the results and revised the manuscript. F.M.-J. designed the study, analyzed the data, and wrote and revised the manuscript. F.M.-J. is the guarantor of this work and, as such, had full access to all the data in the study and takes responsibility for the integrity of the data and the accuracy of the data analysis.

**Prior Presentation.** Parts of this study were presented in abstract form at the Keystone Symposia on Molecular and Cellular Biology: Sex and Gender Factors Affecting Metabolic Homeostasis, Diabetes and Obesity (C6), Tahoe City, CA, 19–22 March 2017.

## References

1. Mauvais-Jarvis F, Clegg DJ, Hevener AL. The role of estrogens in control of energy balance and glucose homeostasis. Endocr Rev 2013;34:309–338

2. Mauvais-Jarvis F, Manson JE, Stevenson JC, Fonseca VA. Menopausal hormone therapy and type 2 diabetes prevention: evidence, mechanisms, and clinical implications. Endocr Rev 2017;38:173–188

3. Heine PA, Taylor JA, Iwamoto GA, Lubahn DB, Cooke PS. Increased adipose tissue in male and female estrogen receptor-alpha knockout mice. Proc Natl Acad Sci U S A 2000;97:12729–12734

4. Riant E, Waget A, Cogo H, Arnal JF, Burcelin R, Gourdy P. Estrogens protect against high-fat diet-induced insulin resistance and glucose intolerance in mice. Endocrinology 2009;150:2109–2117

5. Zhu L, Brown WC, Cai Q, et al. Estrogen treatment after ovariectomy protects against fatty liver and may improve pathway-selective insulin resistance. Diabetes 2013;62:424–434

6. Ribas V, Nguyen MT, Henstridge DC, et al. Impaired oxidative metabolism and inflammation are associated with insulin resistance in ERalpha-deficient mice. Am J Physiol Endocrinol Metab 2010;298:E304–E319
7. Ribas V, Drew BG, Zhou Z, et al. Skeletal muscle action of estrogen receptor α is critical for the maintenance of mitochondrial function and metabolic homeostasis in females. Sci Transl Med 2016;8:334ra54
8. Le May C, Chu K, Hu M, et al. Estrogens protect pancreatic beta-cells from apoptosis and prevent insulin-deficient diabetes mellitus in mice. Proc Natl Acad Sci U S A 2006;103:9232–9237
9. Tiano JP, Delghingaro-Augusto V, Le May C, et al. Estrogen receptor activation reduces lipid synthesis in pancreatic islets and prevents β cell failure in rodent models of type 2 diabetes. J Clin Invest 2011;121:3331–3342
10. Kilic G, Alvarez-Mercado AI, Zarrouki B, et al. The islet estrogen receptor-α is induced by hyperglycemia and protects against oxidative stress-induced insulin-deficient diabetes. PLoS One 2014;9:e87941
11. Arnal JF, Lenfant F, Metivier R, et al. Membrane and nuclear estrogen receptor alpha actions: from tissue specificity to medical implications. Physiol Rev 2017;97:1045–1087
12. Levin ER, Hammes SR. Nuclear receptors outside the nucleus: extranuclear signalling by steroid receptors. Nat Rev Mol Cell Biol 2016;17:783–797
13. Pedram A, Razandi M, Sainson RC, Kim JK, Hughes CC, Levin ER. A conserved mechanism for steroid receptor translocation to the plasma membrane. J Biol Chem 2007;282:22278–22288
14. Pedram A, Razandi M, Lewis M, Hammes S, Levin ER. Membrane-localized estrogen receptor α is required for normal organ development and function. Dev Cell 2014;29:482–490
15. Nanjappa MK, Hess RA, Medrano TI, Locker SH, Levin ER, Cooke PS. Membrane-localized estrogen receptor 1 is required for normal male reproductive development and function in mice. Endocrinology 2016;157:2909–2919
16. Meitzen J, Luoma JI, Boulware MI, et al. Palmitoylation of estrogen receptors is essential for neuronal membrane signaling. Endocrinology 2013;154:4293–4304
17. Adlanmerini M, Solinhac R, Abot A, et al. Mutation of the palmitoylation site of estrogen receptor α in vivo reveals tissue-specific roles for membrane versus nuclear actions. Proc Natl Acad Sci U S A 2014;111:E283–E290
18. Liu S, Le May C, Wong WP, et al. Importance of extranuclear estrogen receptor-alpha and membrane G protein-coupled estrogen receptor in pancreatic islet survival. Diabetes 2009;58:2292–2302
19. Tiano JP, Mauvais-Jarvis F. Molecular mechanisms of estrogen receptors' suppression of lipogenesis in pancreatic β-cells. Endocrinology 2012;153:2997–3005
20. Wong WP, Tiano JP, Liu S, et al. Extranuclear estrogen receptor-alpha stimulates NeuroD1 binding to the insulin promoter and favors insulin synthesis. Proc Natl Acad Sci U S A 2010;107:13057–13062
21. Navarro G, Xu W, Jacobson DA, et al. Extranuclear actions of the androgen receptor enhance glucose-stimulated insulin secretion in the male. Cell Metab 2016;23:837–851
22. Pedram A, Razandi M, Kim JK, et al. Developmental phenotype of a membrane only estrogen receptor alpha (MOER) mouse. J Biol Chem 2009;284:3488–3495
23. Hewitt SC, Kissling GE, Fieselman KE, Jayes FL, Gerrish KE, Korach KS. Biological and biochemical consequences of global deletion of exon 3 from the ER alpha gene. FASEB J 2010;24:4660–4667
24. Fergusson G, Ethier M, Guévremont M, et al. Defective insulin secretory response to intravenous glucose in C57Bl/6J compared to C57Bl/6N mice. Mol Metab 2014;3:848–854
25. Allard C, Carneiro L, Grall S, et al. Hypothalamic astroglial connexins are required for brain glucose sensing-induced insulin secretion. J Cereb Blood Flow Metab 2014;34:339–346
26. Kimura K, Tanida M, Nagata N, et al. Central insulin action activates kupffer cells by suppressing hepatic vagal activation via the nicotinic alpha 7 acetylcholine receptor. Cell Reports 2016;14:2362–2374
27. Smith EP, Boyd J, Frank GR, et al. Estrogen resistance caused by a mutation in the estrogen-receptor gene in a man. N Engl J Med 1994;331:1056–1061
28. Vidal O, Lindberg MK, Hollberg K, et al. Estrogen receptor specificity in the regulation of skeletal growth and maturation in male mice. Proc Natl Acad Sci U S A 2000;97:5474–5479
29. Inoue H, Ogawa W, Asakawa A, et al. Role of hepatic STAT3 in brain-insulin action on hepatic glucose production. Cell Metab 2006;3:267–275
30. Biessels GJ, Reagan LP. Hippocampal insulin resistance and cognitive dysfunction. Nat Rev Neurosci 2015;16:660–671
31. Mauvais-Jarvis F. Role of sex steroids in β cell function, growth, and survival. Trends Endocrinol Metab 2016;27:844–855
32. Rosario W, Singh I, Wautlet A, et al. The brain-to-pancreatic islet neuronal map reveals differential glucose regulation from distinct hypothalamic regions. Diabetes 2016;65:2711–2723
33. Bryzgalova G, Gao H, Ahren B, et al. Evidence that oestrogen receptor-alpha plays an important role in the regulation of glucose homeostasis in mice: insulin sensitivity in the liver. Diabetologia 2006;49:588–597
34. Zhu L, Shi J, Luu TN, et al. Hepatocyte estrogen receptor alpha mediates estrogen action to promote reverse cholesterol transport during Western-type diet feeding. Mol Metab 2018;8:106–116
35. Andrisse S, Childress S, Ma Y, et al. Low-dose dihydrotestosterone drives metabolic dysfunction via cytosolic and nuclear hepatic androgen receptor mechanisms. Endocrinology 2017;158:531–544
36. Könner AC, Janoschek R, Plum L, et al. Insulin action in AgRP-expressing neurons is required for suppression of hepatic glucose production. Cell Metab 2007;5:438–449
37. Shin AC, Filatova N, Lindtner C, et al. Insulin receptor signaling in POMC, but not AgRP, neurons controls adipose tissue insulin action. Diabetes 2017;66:1560–1571
38. Olofsson LE, Pierce AA, Xu AW. Functional requirement of AgRP and NPY neurons in ovarian cycle-dependent regulation of food intake. Proc Natl Acad Sci U S A 2009;106:15932–15937
39. Zhu L, Xu P, Cao X, et al. The ERα-PI3K cascade in proopiomelanocortin progenitor neurons regulates feeding and glucose balance in female mice. Endocrinology 2015;156:4474–4491
40. Qiu J, Bosch MA, Meza C, et al. Estradiol protects proopiomelanocortin neurons against insulin resistance. Endocrinology 2018;159:647–664
41. Kulkarni RN, Brüning JC, Winnay JN, Postic C, Magnuson MA, Kahn CR. Tissue-specific knockout of the insulin receptor in pancreatic beta cells creates an insulin secretory defect similar to that in type 2 diabetes. Cell 1999;96:329–339
42. Mauvais-Jarvis F, Virkamaki A, Michael MD, et al. A model to explore the interaction between muscle insulin resistance and beta-cell dysfunction in the development of type 2 diabetes. Diabetes 2000;49:2126–2134
43. Ward WK, Bolgiano DC, McKnight B, Halter JB, Porte D Jr. Diminished B cell secretory capacity in patients with noninsulin-dependent diabetes mellitus. J Clin Invest 1984;74:1318–1328